Journal of Metallurgy and Materials Science, Vol. 58, No. 3, July-September 2016, pp. 133-146
Printed in India, © NML, ISSN 0972-4257

Numerical modelling of dissipation energy of high tensile steel frames against cyclic earthquake excitations

A.K. DUTTA*, S. SIVAPRASAD, H.N. BAR, P. PRASAD[1] and K. KUMAR[2]
CSIR-National Metallurgical Laboratory, Jamshedpur-831007, India
[1]National Institute of Technology, Jamshedpur, India
[2]CSIR-SERC, Chennai, India

Abstract : The design of steel structures for ductile response requires (a) material ductility, (b) cross section and member ductility, and (c) structural ductility. Dissipating the earthquake input energy by means of plastic excursions has to be compatible with the plastic deformation capacity of the structure. This work concerns incremental approach of modeling for elastoplastic analysis of structural members subjected to harmonically varying severe earthquake loads and their parametric responses over a range of applied frequencies and amplitudes. Investigations have been carried out in respect of stable and reliable hysteretic energy dissipation mechanisms of high rise steel structures against typical time-history loading of four hypothetical frequencies. Eigen-buckling responses for high rise steel structures subjected to earthquake forces are derived using general purpose software (STAAD). Finally critical structural component is identified for the high rise steel structure for estimation of available in-elastic dissipation energy from material ductility against earthquake excitations. The novelty allows for a very useful generalized formulation for the basic analysis procedures adopted in non-linear material problems. All essential features of a non-linear finite element solution are described in relation to one dimensional model for elasto-plastic beam bending. Solutions techniques are programmed in FORTRAN 90 for Newton-Raphson iteration for non-linear finite element analysis to derive hysteretic energy dissipation of high rise steel structures.

Keywords : Steel structure, ductility, dissipation energy, earthquake excitation, finite element method.

INTRODUCTION

Dissipative structures are able to withstand severe earthquakes, by virtue of their ductility and energy dissipation capacity due to ductile hysteretic behavior of some of their components. These components are, therefore, referred to as dissipative zones. Non dissipative part of dissipative seismic structures and their connections to the dissipative ones have to be designed with sufficient over strength in order to allow the cyclic yielding of the dissipative parts. This means that non dissipative parts have to be designed in order to remain within the elastic range and, therefore, they have to be proportioned on the basis of maximum internal actions that the dissipative zones are able to transmit. The fundamental property that makes possible the application of plastic analysis to structural steel design is that the structural material has sufficient ductility. This ductility enables steel structures to reap the benefits of plastification and moment redistribution and leads to higher load carrying capacity. Structural engineers are concerned with the stability of motion in response of high rise structures against random loading from seismic events. Comparatively limited literature exists on the dynamic stability of structures subjected to time-varying random loads. Ductility of structures plays a fundamental role in seismic design. Structures are usually designed so that some of the energy input during severe earthquakes is dissipated through inelastic deformations. The first step of

**Corresponding Authors Email : akd@nmlindia.org*

seismic analysis of structures requires the evaluation of available ductility, while the second is the computation of ductility required by the severest design earthquake. The present study represents a continued effort towards evaluation of plastic deformation capacities of steel member of high rise structure subjected to cyclic loads from four hypothetical time history frequencies. The approach is expected to serve as a promising tool for assessment of dissipation of earthquake input energy through hysteretic behavior of the material. This necessitates a sufficiently accurate modeling of the cyclic behavior so that occurrence of failure is characterized by taking into account all plastic excursions. Based on the information obtained from the monotonic behavior of structural steels, cumulative plastic ductility has been determined, so that occurrence of failure may be established from energy criterion.

Datta[1] performed a series of detailed numerical analysis of stiffened plates subjected to in plane longitudinal compressive load for different aspect ratios in a recent paper. Williamson et. al. had considered three different numerical integration procedures for determining responses of model structures due to complex nature of applied loads and nonlinearity governing equilibrium equation[2]. In their work A. Ghersi et al. [3] had proposed combination of the "N2 method" and the "global" approach to achieve the best dissipative mechanism for steel moment resisting frames. Their proposition formulates a new design method for steel moment resisting frames, combining the N2 method with a design criterion, called "global design method". T.L. Karavasilis, et al.[4] replaced the framed structure by an elastic single degree of freedom substitute structure for which the design displacement, associated with the local damage of the limit state under consideration, had established. Conti M. A.,et.al. [5] in their work has worked out similarities between knee elements of knee braced frames intermediate links of eccentrically braced frames. For an assigned collapse mechanism of a knee braced frame, due to action of diagonal, the knee element is divided into two parts, each one is subjected at its ends to plastic deformations of different values, where moment - shear interaction mechanism is not always negligible. For intermediate knees, moment - shear interaction is significant. In their work Conti M. A.,et.al. [Ref 6] has developed new procedure for calculating the ultimate resistances and corresponding plastic deformations. Conti M. A., et.al.[6] in their work has illustrated a design methodology able to guarantee a collapse mechanism of global type for knee braced frames. They had assumed the beam, brace and knee sections are known, while the column sections constitute the unknowns of the design problem.

In the present study a detailed numerical analysis of high rise steel frame structure is performed to describe the static and dynamic responses of the frame structure subjected to a typical earthquake load. All the frame structures are selected with similar steel grade for columns, floor beams and inclined bracings. The solution technique makes use of interaction between ground acceleration and structural systems through response spectrum. Commercial finite element program STAAD Pro. 2005 has been applied for the modal analysis in order to assess the response history of high rise steel frame structures to a specified ground motion in conjunction with El Centro response spectrum. The number of hysteresis loops upto ultimate tensile stresses for tensile structural steels have been derived by FORTRAN coding. Finally numerical methods have been explained and coding in FORTRAN 90 generated for Newton-Raphson iteration for non-linear analysis to determine cumulative dissipation energy of critical member of high rise steel structures.

Model High Rise Steel Frame Structure

Case studies are made for determining mode shapes of steel frame structure with three different ranges of number of storey (10 nos., 20 nos., & 30 nos.) with storey height of 3.5 m. The frame structures are subjected to a typical time history loading from El Centro time history

earthquake excitations [Fig. 1]. Finite element model for number of storey 10 is shown in Figs. 2, 3 & 4. The dead loads and live loads are calculated according to the data found from design documents for each floor. A series of detailed numerical analysis are performed to describe the static and dynamic responses of high rise steel frame structure square layout plan (12.4m x 12.4 m). The columns (ISHB 450 X 250 X 11.3) and floor beams (ISHB 400 X 250 X 10.6) of the structures are selected with A36 grade steel. Inclined bracings are provided with ISMC 250. The control is based on modification of the dynamic characteristics in which the structural period is shifted away from the predominant periods of seismic input, thus avoiding the risk of resonance occurrence. Commercial finite element program STAAD Pro. 2005 has been applied for the modal analysis in order to assess the response history of high rise steel frame structures to the specified ground motion.

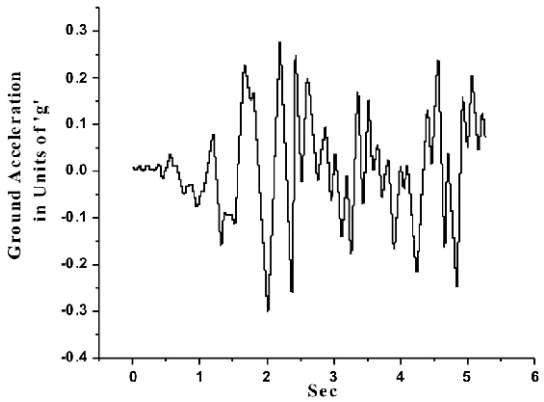

Fig. 1 : Ground Motion in El Centro, California Earthquake of May, 1940

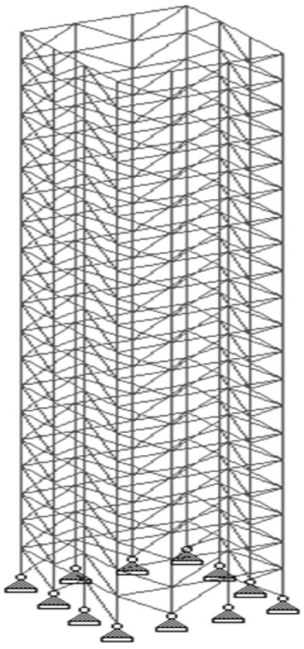

Fig. 2 : Model 10 Storey Square Frame Structure

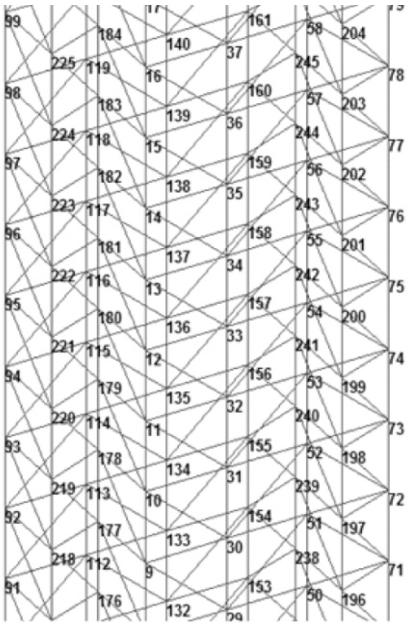

Fig. 3 : Part Model 10 Storey Square Frame Structure with generated node numbers

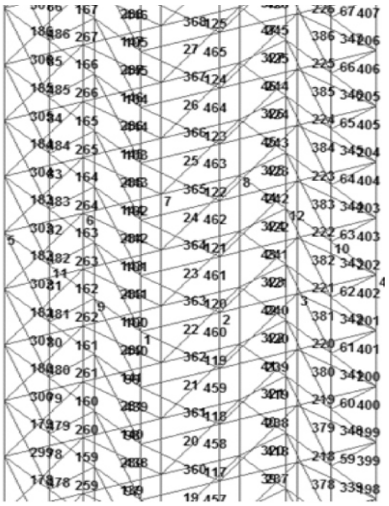

Fig. 4 : Part Model 10 Storey Square Frame Structure with generated members

	Beam	L/C	Node	Fx kg	Fy kg	Fz kg	Mx kNm	My kNm	Mz kNm
Max Fx	3	5 STATIC + NEGATIVE DYNAMIC	23	1.83E+05	-272.633	-4.639	0	0	0
Min Fx	182	5 STATIC + NEGATIVE DYNAMIC	33	-1.76E+05	-252.31	17.604	-0.009	0.691	6.749
Max Fy	31	5 STATIC + NEGATIVE DYNAMIC	21	1.07E+05	1.06E+05	837.164	0.034	-18.648	2174.369
Min Fy	23	4 STATIC + POSITIVE DYNAMIC	24	-85236.599	-83164.946	-40.555	0.107	4.799	1328.735
Max Fz	65	4 STATIC + POSITIVE DYNAMIC	70	-18470.495	-12350.787	1009.909	0.108	14.427	-671.734
Min Fz	74	5 STATIC + NEGATIVE DYNAMIC	36	-21464.914	28714.73	-1670.73	0.388	51.498	102.892
Max Mx	74	5 STATIC + NEGATIVE DYNAMIC	36	-21464.914	28714.73	-1670.73	0.388	51.498	102.892
Min Mx	111	4 STATIC + POSITIVE DYNAMIC	10	884.781	18284.267	-1236.06	-0.468	53.777	0.188
Max My	66	4 STATIC + POSITIVE DYNAMIC	82	-16333.463	-12737.174	993.224	0.031	57.404	21.009
Min My	45	4 STATIC + POSITIVE DYNAMIC	48	-32244.386	-29855.734	859.711	0.234	-62.094	-111.459
Max Mz	21	4 STATIC + POSITIVE DYNAMIC	21	37979.801	-64658.074	865.772	0.101	-18.358	2210.266
Min Mz	113	4 STATIC + POSITIVE DYNAMIC	112	-1.21E+05	63197.989	-604.482	-0.121	6.074	-1973.93

Fig. 5 : Staad Pro Output for Model 10 Storey Square Frame Structure

	Beam	L/C	Node	Fx kg	Fy kg	Fz kg	Mx kNm	My kNm	Mz kNm
Max Fx	12	4 STATIC + POSITIVE DYNAMIC	232	2.77E+05	3.037	-5.256	0	0	0
Min Fx	153	4 STATIC + POSITIVE DYNAMIC	170	-2.82E+05	1.44E+05	-91.457	-0.239	2.143	2452.456
Max Fy	154	4 STATIC + POSITIVE DYNAMIC	171	-1.20E+05	1.63E+05	37.437	-0.367	-0.717	3350.905
Min Fy	214	5 STATIC + NEGATIVE DYNAMIC	234	-1.20E+05	-1.63E+05	37.437	-0.367	0.717	3350.905
Max Fz	334	5 STATIC + NEGATIVE DYNAMIC	65	1.67E+05	6130.166	273.221	0.148	-10.093	203.282
Min Fz	454	5 STATIC + NEGATIVE DYNAMIC	128	76012.039	8293.985	-262.281	0.146	4.146	168.368
Max Mx	14	4 STATIC + POSITIVE DYNAMIC	3	-52570.055	78453.881	212.3	0.672	-5.848	273.252
Min Mx	150	4 STATIC + POSITIVE DYNAMIC	19	60106.097	75947.491	194.552	-0.626	-5.035	256.006
Max My	8	4 STATIC + POSITIVE DYNAMIC	168	62438.953	-27.712	30.347	0.007	20.759	19.005
Min My	1	5 STATIC + NEGATIVE DYNAMIC	21	62438.953	27.712	-30.347	0.007	-20.759	-19.005
Max Mz	234	5 STATIC + NEGATIVE DYNAMIC	234	-67015.819	98098.909	-228.368	0.597	6.146	3463.566
Min Mz	173	4 STATIC + POSITIVE DYNAMIC	212	-1.59E+05	-80322.867	165.942	0.461	-6.912	-3174.15

Fig. 6 : Staad Pro Output for Model 20 Storey Square Frame Structure

	Beam	L/C	Node	Fx kg	Fy kg	Fz kg	Mx kNm	My kNm	Mz kNm
Max Fx	553	5 STATIC + NEGATIVE DYNAMIC	280	4.06E+05	8358.375	16.421	-0.001	-1.011	192.53
Min Fx	313	5 STATIC + NEGATIVE DYNAMIC	281	-4.34E+05	-2.00E+05	-142.735	-0.375	2.437	-4699.44
Max Fy	224	4 STATIC + POSITIVE DYNAMIC	251	-1.98E+05	2.57E+05	54.182	-0.594	-1.09	5338.037
Min Fy	314	5 STATIC + NEGATIVE DYNAMIC	344	-1.98E+05	-2.57E+05	54.183	-0.594	1.092	5338.037
Max Fz	494	5 STATIC + NEGATIVE DYNAMIC	95	2.59E+05	9365.016	427.402	0.231	-15.762	314.591
Min Fz	524	4 STATIC + POSITIVE DYNAMIC	33	1.27E+05	13390.243	-414.163	0.23	6.542	271.135
Max Mx	14	4 STATIC + POSITIVE DYNAMIC	3	-87777.861	1.27E+05	345.141	1.081	-9.219	444.08
Min Mx	220	4 STATIC + POSITIVE DYNAMIC	29	1.04E+05	1.24E+05	312.923	-1.002	-7.549	415.063
Max My	8	4 STATIC + POSITIVE DYNAMIC	248	1.03E+05	-25.333	30.369	0.008	28.557	26.057
Min My	1	5 STATIC + NEGATIVE DYNAMIC	31	1.03E+05	25.333	-30.369	0.008	-28.557	-26.057
Max Mz	194	4 STATIC + POSITIVE DYNAMIC	251	-1.10E+05	-1.53E+05	-366.532	0.966	-9.575	5500.35
Min Mz	253	4 STATIC + POSITIVE DYNAMIC	312	-2.44E+05	-1.29E+05	262.554	0.723	-10.891	-4981.68

Fig. 7 : Staad Pro Output for Model 30 Storey Square Frame Structure

Output from STAAD Pro.

Responses of high rise frame structures subjected to time-history earthquake loads on model frames are presented in Figs. 5, 6 & 7. Finally cumulative dissipation energies have been evaluated from non-linear analysis applying Newton-Raphson iteration technique for critical members.

Dissipation Energy of Steels under Repeated Cyclic Loading

A most important property of steels subjected to cyclic inelastic loading is their ability to dissipate hysteretic energy. The energy needed to plastically elongate or shorten a steel specimen can be calculated as the product of the plastic force times the plastic displacement (i.e., the work done in the plastic range) and is called the hysteretic energy. Unlike kinetic and strain energy, hysteretic energy is a non-recoverable dissipated energy. Under a progressively increasing loading, followed by subsequent unloading, the hysteretic energy, E_H, can be expressed as [Fig. 8] :

$$E_H = P_Y (\delta_{max} - \delta_Y) \quad ...(1)$$

For a full cycle load reversal, the hysteretic energy will simply be the area enclosed by the loop of the force- displacement curve, and approximately expressed as [Fig. 8] :

$$E_H = P_Y (\delta_{max} - \delta_Y) + (\delta_{max} - \delta_{min} - 2\delta_Y) \quad ...(2)$$

A more accurate calculation of hysteretic energy in this case would recognize the small loss of hysteretic energy at the rounded corners of the force- displacement curve due to Bouchinger effect. Under repeated cycles of loading, the energy dissipated in each cycle is simply summed to calculate the total energy dissipated. The cumulative energy dissipation capacity is a most important property that makes possible survival of steel structures to rare but rather severe loading conditions. As steel undergoes numerous cycles of severe hysteretic behavior, the threshold beyond which strain hardening starts to develop, as well as the extent of elastic range prior to the onset of Bouchinger effect, is a function of the prior plastic loading history[Fig. 9]. In this study stress~strain curve for commercially available structural steel grade A36 is taken from Laboratory test data with a particular emphasis on its desirable ductile properties. From this steel property cumulative energy dissipation capacity has been evaluated three hypothetical time history loadings. Numerical analysis has been carried out by Fortran coding for generation of hysteresis loops within available ductile zones of respective stress~strain curves upto maximum load of strain hardening capacity.

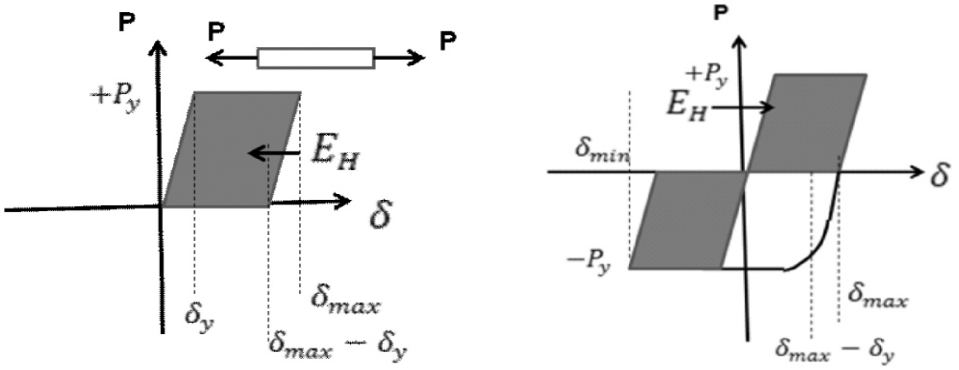

Fig. 8 : Hysteretic Energy of Structural Steel

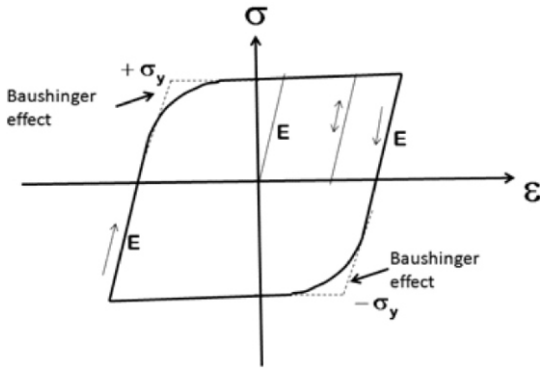

Fig. 9 : Cyclic Stress-Strain Relationship of Structural Steel

Derivation of Dissipation Energy Curves

The focus of this study is on developing a better understanding of the response of high rise steel structures and the assessment of the energy absorbing capacities for a wide range of frequencies of ground motions. Ground motions of different frequencies will result in different strain increments in the plastic zone of the stress-strain curve. Thus characteristics of hysteretic Loops for cyclic earthquake excitations will be different for respective strain increments in the plastic zone of the stress-strain curve. Thus the approach consists of a step-by-step direct integration in which the domain is discretized into a large number of small increments. For each time interval equation of motion is solved to obtain the structural responses such as displacements.

Stress-strain curves from Laboratory test data have been plotted in Fig. 10 for tensile structural steels A36. Available ductility zones are of significant importance for characterization of hysteretic dissipation energy available for different grades of structural steels from earthquake excitations. However, responses are also studied in respect of four hypothetical strain increments with respect to corresponding repeated cyclic loading. A program 'LOOP' in FORTRAN 90 coding has been developed to generate stress-strain data from cyclic responses of four hypothetical strain increments of 0.0015, 0.002, 0.0025 and 0.003. The characteristics of hysteretic Loops for respective strain increments have been clearly manifested in Figs. 11-14.

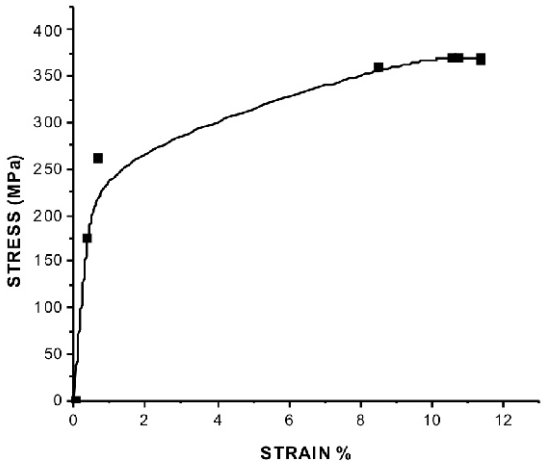

Fig. 10 : Stress- Strain Curve for A36 Grade Steel

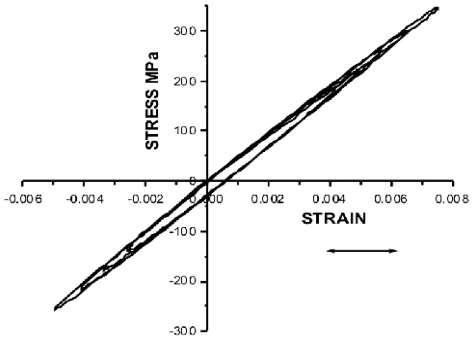

Fig. 11 : Hysteretic Loop for Cyclic Earthquake Excitation for Strain Increment 0.0015 Steel Grade A36

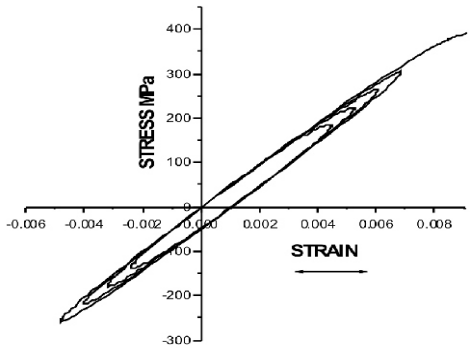

Fig. 12 : Hysteretic Loop for Cyclic Earthquake Excitation for Strain Increment 0.002 Steel Grade A36

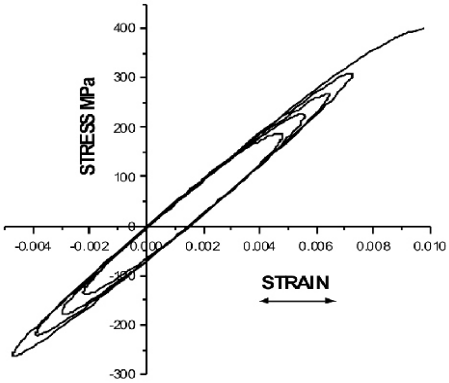

Fig. 13 : Hysteretic Loop for Cyclic Earthquake Excitation for Strain Increment 0.0025 Steel Grade A36

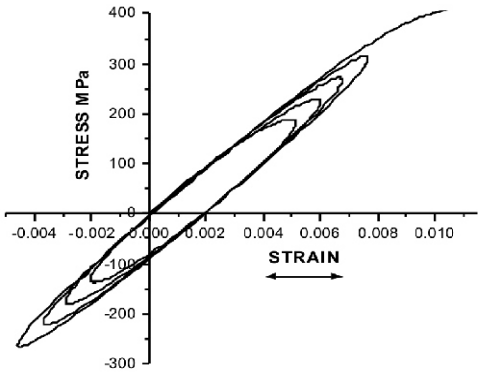

Fig. 14 : Hysteretic Loop for Cyclic Earthquake Excitation for Strain Increment 0.003 Steel Grade A36

Modular approach of modeling for nonlinear problems

A modular approach is adopted and separate subroutines are employed to perform the various operations required in a nonlinear finite element analysis to account all plastic excursions [Fig. 15].

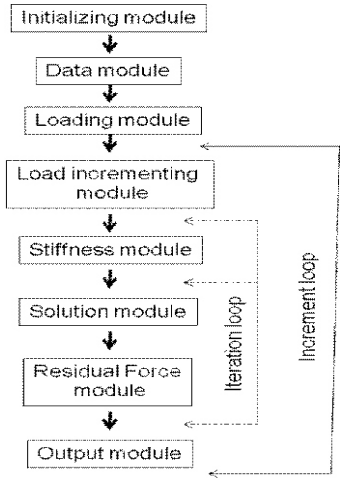

Fig. 15 : Program module for nonlinear solution code

– Initializing module is the first module entered and its function is to initialize to zero various vectors and matrices at the beginning of the solution process.

– Data input module handles input data defining the geometry, boundary conditions and material properties. This data is checked using diagnostic routines and if errors occur, they are flagged. For isoparametric elements, Gaussian integration constants and mid-side nodal coordinates for straight sided elements are also evaluated in this solution.

– Loading module organizes the calculation of nodal forces due to various forms of loading.

– Load increment module controls the incrementing of applied loads evaluated by the loading module.

– Stiffness module organizes the evaluation of stiffness matrix for each element. The stiffness matrices are stored in a disc and ordered in a sequence required for equation assembly and reduction.

– Solution module organizes the assembly, reductions and solution of the governing set of simultaneous equations to give the nodal displacements and force reations.

– Residual force module calculates the residual or out of balance nodal forces at each stage of the analysis.

– Output module organizes the output of the requested quantities.

Solution of nonlinear equations

Now nonlinear equilibrium equations will be generated using virtual work expression. At any point in finite element mesh the lateral displacement and rotation can be obtained from the expression :

$$\begin{bmatrix} W \\ \theta \end{bmatrix} = N\varphi \qquad ...(3)$$

The shape function matrix is as follows :

$$N = \begin{bmatrix} N_1 & 0 & N_2 & 0 & ..... & N_n & 0 \\ 0 & N_1 & 0 & N_2 & ..... & 0 & N_n \end{bmatrix} \qquad ...(4)$$

The vector of nodal displacements:

$$\varphi = [W_1 \ \theta_1 \ W_2 \ \theta_2 ..... W_n \ \theta_n]^T \qquad ...(5)$$

Where w_i, θ_i and N_i are the lateral displacement, rotation and global shape functions associated with node 'i'.

The curvature and shear strain at any point within the entire finite element mesh is given as :

$$-\frac{d\theta}{dx} = B_f \varphi \qquad \frac{dw}{dx} - \theta = B_s \varphi \qquad ...(6)$$

Where

$$B_f = \left[0 \ -\frac{dN_1}{dx} \ 0 \ -\frac{dN_2}{dx} \ ..... \ 0 \ -\frac{dN_n}{dx} \right] \qquad ...(7)$$

$$B_s = \left[\frac{dN_1}{dx} - N_1 \ \frac{dN_2}{dx} - N_2 \ ..... \ \frac{dN_n}{dx} - N_n \right] \qquad ...(8)$$

Virtual curvatures and shear strains are given as :

$$-\frac{d(\delta\theta)}{dx} = B_f\ \delta\varphi \qquad \frac{d(\delta w)}{dx} - \delta\theta = B_s\ \delta\varphi \qquad ...(9)$$

The vector of virtual nodal displacements is written as :

$$\delta\varphi = \left[\delta w_1\ \ \delta\theta_1\ \ \delta w_2\ \ \delta\theta_2\ \ .....\ \ \delta w_n\ \ \delta\theta_n\right]^T \qquad ...(10)$$

The virtual work expression can now be ex[pressed as :

$$\int_0^l \left[\delta\varphi\right]^T \left[B_f\right]^T M\ dx + \int_0^l \left[\delta\varphi\right]^T \left[B_s\right]^T Q\ dx$$

$$-\int_0^l \left[\delta\varphi\right]^T \left[\overline{N}\right]^T q\ dx = 0 \qquad ...(11)$$

$$\overline{N} = \left[N_1\ \ 0\ \ N_2\ \ 0\ .....\ N_n\ 0\right] \qquad ...(12s)$$

From (11.9) for any set of virtual displacement $\delta\varphi$:

$$\left\{\int_0^l \left[B_f\right]^T M\ dx + \int_0^l \left[B_s\right]^T Q\ dx\right\} - \int_0^l \left[\overline{N}\right]^T q\ dx = 0 \qquad ...(13)$$

Or p - f = 0

In elasto-plastic problem 'M' is a nonlinear function and in general the vector 'p' is predicted only approximately. Thus in (13) p-f will equal to a residual value $\varepsilon(\varphi)$ which will be reduced to zero in the solution process.

Thus contribution from element 'e' to the matrix 'p' is given by :

$$p^{(e)} = \int_{x_1^{(e)}}^{x_2^{(e)}} \begin{bmatrix} 0 \\ \frac{1}{l^{(e)}} \\ 0 \\ -\frac{1}{l^{(e)}} \end{bmatrix} M^{(e)} dx + \int_{x_1^{(e)}}^{x_2^{(e)}} \begin{bmatrix} -\frac{1}{l^{(e)}} \\ \frac{x^{(e)} - x_2^{(e)}}{l^{(e)}} \\ \frac{1}{l^{(e)}} \\ \frac{x_1^{(e)} - x^{(e)}}{l^{(e)}} \end{bmatrix} Q^{(e)} dx \qquad ...(14)$$

$$= \left[-\ Q^{(e)}\ \ M^{(e)} - \frac{(Ql)^{(e)}}{2}\ \ Q^{(e)}\ \ -M^{(e)} - \frac{(Ql)^{(e)}}{2}\right]^T$$

Derivation of dissipation energy

A program 'DISSIPATION' in FORTRAN 90 coding for structural system has been established for numerical analysis of the critical beam members of respective high rise steel structures models. The same is based on the constitutive relationship for the critical beam member as well as finite element type. Following basic principles are adopted in the proposed non-linear solution:

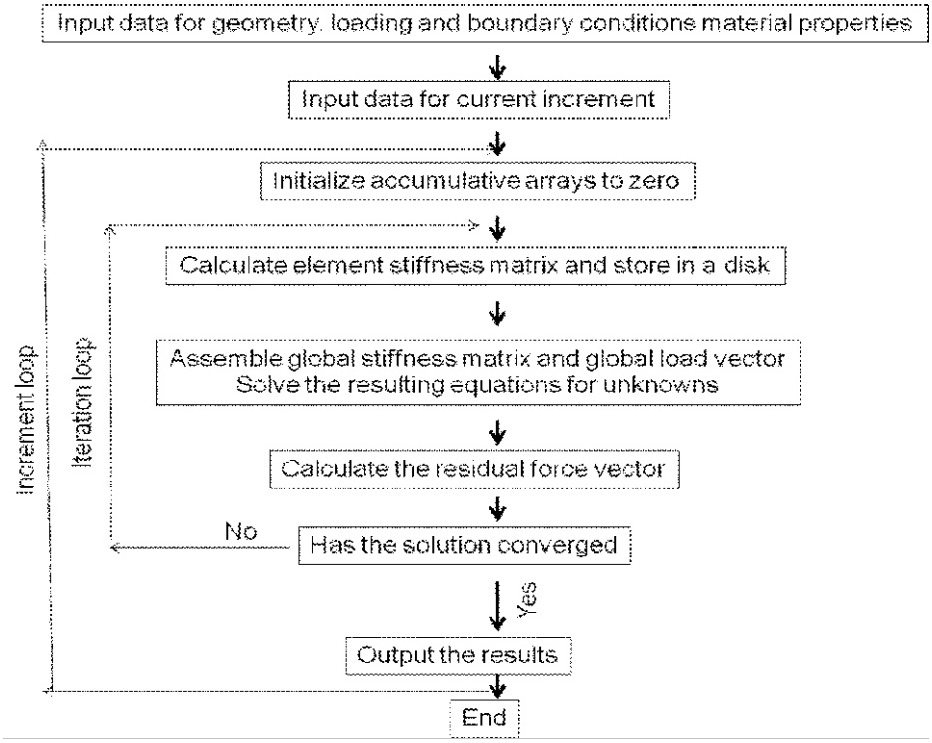

Fig. 15 : Overall structural program elasto-plastic Timoshenko Beam

The program reads the respective stress-strain data from cyclic responses of four strain increments of 0.0015, 0.002, 0.0025 and 0.003.

Total numbers of cycles are evaluated for respective stress-strain data from cyclic responses.

– Newton-Raphson iteration for non-linear finite element analysis is executed for each cycle for the critical beam member with moments and shear generated from STAAD Pro solutions.

– Each cycle is solved for six increments of beam loads with fifty iterations. Iterations stopped where convergence is attained within tolerance limit.

– The output is saved in a file generated by the program 'DISSIPATION'. A typical output from program is shown in Fig. 17 for strain increment 0.003. The output shows final 50th iteration results for each load increment of cycle 1 only.

– The program reads final rotation of the fixed end for each cycle from the saved data file. Finally energy absorption capacity is evaluated by multiplying critical moment with cumulative rotation from successive cycles of the said strain increment. Typical FORTRAN output for rotations from successive cycles after 50 Newton-Raphson iteration for strain increment 0.003 is shown in Fig. 16.

DISCUSSION

The fundamental property that makes possible the application of plastic analysis to structural steel design is that the structural material has sufficient ductility. This ductility enables steel structures to reap the benefits of plastification and moment redistribution and leads to higher energy absorbing capacity.

```
ROTATION IN RAD SUCCESSIVE CYCLE =       .6894590E+00
ROTATION IN RAD SUCCESSIVE CYCLE =       .7687440E+00
ROTATION IN RAD SUCCESS  IVE CYCLE =     .6894590E+00
ROTATION IN RAD SUCCESSIVE CYCLE =       .5047620E+00
ROTATION IN RAD SUCCESSIVE CYCLE =       .6918450E+00
ROTATION IN RAD SUCCESSIVE CYCLE =       .7456330E+00
ROTATION IN RAD SUCCESSIVE CYCLE =       .6937270E+00
ROTA TION IN RAD SUCCESSIVE CYCLE =      .5532150E+00
ROTATION IN RAD SUCCESSIVE CYCLE =       .6896430E+00
ROTATION IN RAD SUCCESSIVE CYCLE =       .7205320E+00
ROTATION IN RAD SUCCESSIVE CYCLE =       .6862720E+00
ROTATION IN RAD SUCCESSIVE CYCLE =       .5719220E+00
ROTATION IN RAD SUCCESSIVE CYCLE =       .6881470E+00
ROTATION IN RAD SUCCESSIVE CYCLE =       .7104840E+00
ROTATION IN RAD SUCCESSIVE CYCLE =       .6897450E+00
ROTATION IN RAD SUCCESSIVE CYCLE =       .5940340E+00
ROTATION IN RAD SUCCE  SSIVE CYCLE =     .6911210E+00
ROTATION IN RAD SUCCESS  IVE CYCLE =     .6552940E+00

TOTAL DISSIPATION ENERGY =   .4885819E+09
```

Fig. 16 : Typical FORTRAN Output for Rotations from Successive Cycles after 50 Newton-Raphson Iteration for Strain Increment 0.003 [Steel Grade A36]

```
CYCLE NO:     EIVAL         SVALU      YIELD MOMENT     HARDS
   1      .14000E+07     .19938E+08     .25200E+05     .31292E+10

0   IINCS=   1  NITER=  50  NOUTP=   2  FACTO=      .050000  TOLER=
.500000
0   NODE          DISPL        REACTIONS        DISPL.         REACTION
      1       .000000E+00      -.714404E-38      .000000E+00      -.142842E+05
      2       .510380E-02      .000000E+00       .10 2076E-01     .000000E+00
      3       .204152E-01      .000000E+00       .204152E -01     .000000E+00
      4       .447790E-01      .000000E+00       .283125E -01     .000000E+00

0   IINCS=   2  NITER=  50  NOUTP=    2  FACTO=      .100000  TOLER=
.500000
0   NODE          DISPL        REACTIONS        DISPL.         REACTION
      1       .000000E+00      .139697E -37      .000000E+00      -.428527E+05
      2       .159915 E-01     .000000E+00       .319831E -01     .000000E+00
      3       .639662E-01      .000000E+00       .639662E -01     .000000E+00
      4       .140305E+00      .000000E+00       .887107E  -01      .000000E+00

0   IINCS=   3  NITER=  50  NOUTP=   2  FACTO=      .150000  TOLER=
.500000
0   NODE          DISPL        REACTIONS        DISPL.         REACTION
      1       .000000E+00      -.139697E-37      .000000E+00      -.857054E+05
      2       .333503E-01      .000000E+00       .667005E  -01     .000000E+00
      3       .133401E+00      .000000E+00       .133401E+00      .000000E+00
      4       .292604E+00      .000000E+00       .1850  06E+00      .000000E+00

0   IINCS=   4  NITER=  50  NOUTP=   2  FACTO=      .200000  TOLER=
.500000
0   NODE          DISPL        REACTIONS        DISPL.         REACTION
      1       .000000E+00      .91083 0E-38      .000000E+00      -.142842E+06
      2       .578647E-01      .000000E+00       .115729E+00      .000000E+00
      3       .231459E+00      .000000E+00       .231459E+00      .000000E+00
      4       .507686E+ 00      .000000E+00       .320996E+00      .000000E+00

0   IINCS=   5  NITER=  50  NOUTP=   2  FACTO=      .250000  TOLER=
.500000
0   NODE          DISPL        REACTIONS        DISPL.         REACTION
      1       .000000E+00      .000000E+00       .000000E+00       -.214263E+06
      2       .902196E-01      .000000E+00       .180439E+00      .000000E+00
      3       .360878E+00      .000000E+00       .360878E+00      .000  000E+00
      4       .791557E+00      .000000E+00       .500479E+00      .000000E+00

0   IINCS=   6  NITER=  50  NOUTP=   2  FACTO=      .250000  TOLER=
.500000
0   NODE          DISPL        REACTIONS          DISPL.         REACTION
      1       .000000E+00      .114906E -38      .000000E+00      -.285685E+06
      2       .124286E+00      .000000E+00       .248573E+00      .000000E+00
      3       .497145E+00      .000000E +00       .497145E+00      .000000E+00
      4     .109045E+01      .000000E+00      .689459E+00      .000000E+00
```

Fig. 17 : Typical FORTRAN Output for Newton-Raphson Iteration for non-linear finite element Analysis Cycle 1 for Strain Increment 0.003 [Steel Grade A36]

This research presents a numerical study on the estimation of dynamic characteristics of high rise steel structures against seismic excitations. Hysteretic dissipation energy and hence the energy absorption capacity responses for varying storey heights and incremental strains in cyclic stress-strain curves for steel frame structures are shown in Figs. 18-22. Remarkable dissipation energy capacities have been indicated for each storey height supporting second level of seismic performance and the structure does not collapse under a severe earthquake event. However the dissipation energy capacities exhibit monotonic decrease with increase in incremental strains and hence time period of seismic load for a particular storey height. However values of these decreases in dissipation energy capacities are very limited for a storey height as shown in Figs. 19-22. Height of steel frame structure has considerable impact on energy absorption capacities against seismic response. The value of dissipation energies increases remarkably as storey height increase for frame structures with square layout area [Figs. 18 & 22]. It is evident from Figs. 18 & 22 that rate of increase is higher as number of storey increases. However the slope decreases after certain height. This is unique finding from this study and it ensures that there is certainly optimized height where there will be maximum value of dissipation energy for high rise structures.

Responses are studied in respect of four different hypothetical strain increments in the plastic zone of the stress-strain curve. Each strain increment corresponds to a ground motion of particular frequency. with respect to corresponding repeated cyclic loading. Data from cyclic stress-strain responses of four hypothetical strain increments are generated from FORTRAN coding.

Available hysteretic dissipation energies from typical cyclic stress strain responses for steel elements for hypothetical strain increments are shown in Figs 11-14.

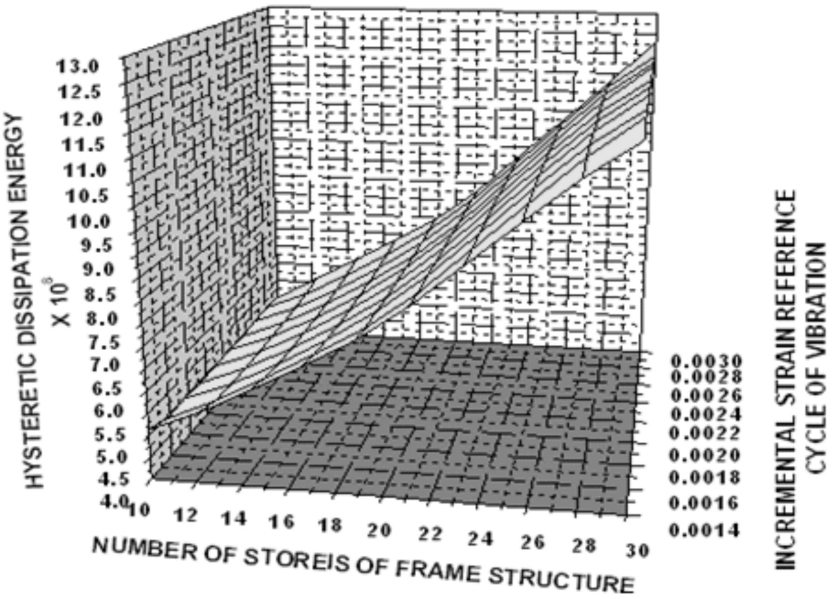

Fig. 18 : Response Dissipation Energy of AS 36 Steel for Incremental Strain Reference Cyclic Loading from and Number of Stories

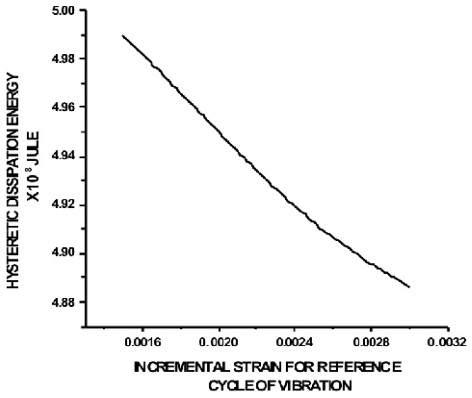

Fig. 19 : Response Dissipation Energy of AS 36 Steel for Incremental Strain Reference Cyclic Loading for 10 Number of Stories

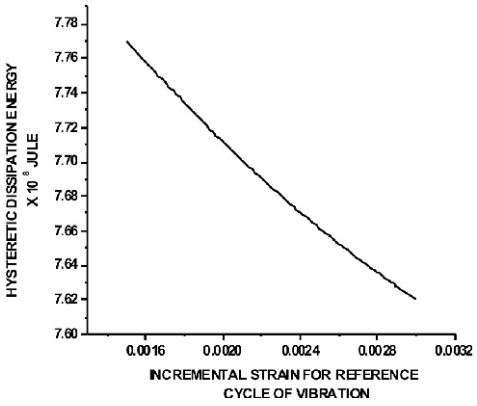

Fig. 20 : Response Dissipation Energy of AS 36 Steel for Incremental Strain Reference Cyclic Loading for 20 Number of Stories

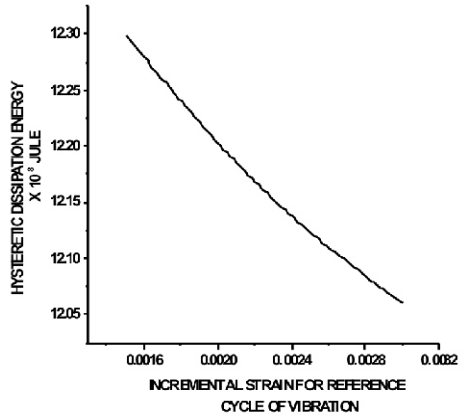

Fig. 21 : Response Dissipation Energy of AS 36 Steel for Incremental Strain Reference Cyclic Loading for 30 Number of Stories

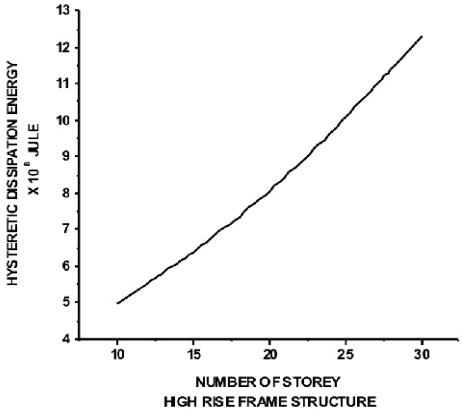

Fig. 22 : Response Dissipation Energy of AS 36 Steel for Incremental Strain Reference Cyclic Loading against Number of Stories

The specimens exhibit large stable hysteresis loops, and a strength increase of almost 40% - 55% above yield on account of cyclic strain hardening. As is evident A36 have considerable shock absorbing capacity from repeated cyclic loading with larger ductile domain. Increasing energy capacities are depicted with increasing strain

High tensile steel AS 514 has maximum ultimate tensile stress but very limited ductile zone compared to A36 and AS314. AS 514 steel has limited energy absorbing capacity from repeated cyclic loading from earthquake excitations. Rather it has fast decreasing hysteretic energy capacity as period of vibration increases. Steel columns are normally designed as non-dissipative part of dissipative seismic structures. These are designated as strong columns while connecting steel beams are designed as dissipative ones for a general weak beam and strong column proposition to avoid collapse. Columns have to be designed with sufficient over strength in order to allow the cyclic yielding of the dissipative parts. Thus beam components and column components of high rise steel structures with AS 304 and with AS 514 respectively will ensure minimum damage from severe earthquake shocks.

CONCLUSION

The fundamental property that makes possible the application of plastic analysis to structural steel design is that the structural material has sufficient ductility. This ductility enables steel structures to reap the benefits of plastification and moment redistribution and leads to higher energy absorbing capacity. Elastic loading and unloading do not effect the stress-strain relationship of steel. However, when steel is unloaded after the yield strain is greatly exceeded, reloading may give a stress-strain relationship different from that observed during the initial loading thus causing a significant reduction in the available ductility. Structures designed according to current seismic code provisions are expected to deform in the inelastic range when subjected to design level earthquake ground motions. The elements of structures are thus called upon to dissipate the seismic energy in the form of hysteretic energy. The ability of structural steel as a base material to dissipate large amount of seismic energy through inelastic deformations makes steel a material ideally suited for structures undergoing seismic excitations. Steel hardens under cyclic loading and gains strength as the number of cycles and the deformation amplitude increase, resulting in large hysteretic loop.

For earthquake resistant design, a structure should meet performance requirements at two different levels, depending upon the magnitude of earthquake actions. The first level of performance essentially requires structural response in the elastic range without significant structural damage under moderate earthquake action, and the second level of performance requires that the structure does not collapse under a severe earthquake event. The object of this work is to describe computer implementation of nonlinear finite element method to the solution of materially nonlinear engineering problems towards evaluation of plastic deformation capacities of high tensile steel subjected to cyclic loads from seismic excitations. For structures subjected to seismic loading, nonlinear material response results from elasto-plastic material behavior as well as from hyperelastic behavior of some form. In this work essential feature of nonlinear finite element solution is described in relation to one dimensional models of elasto-plastic beam bending. Solution techniques are programmed in FORTRAN 90 and numerical elasto-plastic beams are solved for dissipated energy from earthquake excitations through hysteretic behavior of the material. This necessitates a sufficiently accurate modeling of the cyclic behavior so that occurrence of failure is characterized by taking into account all plastic excursions. Based on the information obtained from the monotonic behavior of structural steels, cumulative plastic ductility has been determined, so that occurrence of failure may be established from energy criterion. The approach is expected to serve as a promising tool for assessment of the ability of structures to sustain plastic deformations so that earthquake input energy is dissipated through hysteretic behavior of the material.

REFERENCES

[1] Datta A.K., (2009), Buckling Modes and Optimal Stiffener Arrangement of Rectangular Stiffened Plates under Uniform Lateral Loads', ICASS '09 Sixth Int. Conf. on Advances in Steel Structures, Hong Kong, pp. 16-18.

[2] Williamson E.B., (2002), Rungamornrat J, "Numerical Analysis of Dynamic Stability under Random Excitation", Engineering Structures, **24**, pp. 479 - 490.

[3] Ghersi E.M. Marino and Neri F., A seismic design method for high ductility steel frames, Department of Structural and Environmental Engineering, University of Catania, Catania, Italy.

[4] Karavasilis T.L., Bazeos N. and Beskos D.E., A hybrid force/displacement seismic design method for plane steel frames", Department of Civil Engineering, University of Patras, Patras, Greece.

[5] Conti M.A., Mastrandea L. and Piluso V., (2006), Theoretical analysis of moment shear interaction in knee braced frames', Proceedings of the fifth International Conference on Behaviour of Steel Structures in Seismic Areas, STESSA, pp. 407.

[6] Conti M.A., Mastrandea L. and Piluso V., (2006), Plastic design of seismic resistant knee braced frames', Proceedings of the fifth International Conference on Behaviour of Steel Structures in Seismic Areas, STESSA, pp. 415.